Structural Basis for Feedback Inhibition of the Deoxyribonucleoside Salvage Pathway: Studies of the Drosophila Deoxyribonucleoside Kinase†

Nils Egil Mikkelsen,‡ Kenth Johansson,‡ Andreas Karlsson,‡ Wolfgang Knecht,§,⊥ Gorm Andersen,|| Jure Piškur,§ Birgitte Munch-Petersen,|| and Hans Eklund*,‡

Department of Molecular Biology, Swedish University of Agricultural Sciences, Box 590, Biomedical Center, S-751 24 Uppsala, Sweden, and BioCentrum-DTU, Building 301, Technical University of Denmark, DK-2800 Lyngby, Denmark, and Department of Life Sciences and Chemistry, Roskilde University, DK-4000 Roskilde, Denmark

Received January 3, 2003; Revised Manuscript Received March 25, 2003

ABSTRACT: Deoxyribonucleoside kinases are feedback inhibited by the final products of the salvage pathway, the deoxyribonucleoside triphosphates. In the present study, the mechanism of feedback inhibition is presented based on the crystal structure of a complex between the fruit fly deoxyribonucleoside kinase and its feedback inhibitor deoxythymidine triphosphate. The inhibitor was found to be bound as a bisubstrate inhibitor with its nucleoside part in the nucleoside binding site and with its phosphate groups partially occupying the phosphate donor site. The overall structure of the enzyme−inhibitor complex is very similar to the enzyme−substrate complexes with deoxythymidine and deoxycytidine, except for a conformational change within a region otherwise directly involved in catalysis. This conformational change involves a magnesium ion, which is coordinated in the inhibitor complex to the phosphates and to the primary base, Glu52, that normally is positioned close to the 5′-OH of the substrate deoxyribose.

DNA synthesis is dependent on the abundance of precursor deoxyribonucleoside triphosphates (dNTPs). dNTPs are synthesized either de novo (*1*), or obtained by the salvage pathway by the phosphorylation of deoxyribonucleosides originating from intra- or extracellular breakdown of DNA (*2*). The initial step of the pathway is carried out by deoxyribonucleoside kinases, which catalyze the phosphoryl transfer from a phosphate donor (ATP or other ribonucleoside triphosphates) to deoxyribonucleosides, thereby forming deoxyribonucleoside monophosphates (dNMPs) (*2* and references therein). The dNMPs are further phosphorylated to dNDPs and finally to dNTPs, which can then be utilized in DNA synthesis.

Feedback regulation of enzyme activities plays a major role in the control of many metabolic pathways. In nucleotide metabolism, ribonucleotide reductase is the key enzyme in the de novo formation of DNA precursor dNTPs and its activity and specificity is highly regulated by dNTPs (*3* and references therein). Similarly, dNTPs also regulate the salvage pathway, as several of the deoxyribonucleoside kinases are feedback regulated by the end-product, deoxyribonucleoside triphosphates (*4*−*8*). The most potent inhibitors are usually the triphosphates of the preferred substrates.

Balanced nucleotide pools are of crucial importance for the proper function of a cell or organism. The necessity of finely regulated deoxyribonucleoside kinase function is emphasized by the recent findings that mutations causing lower activity of human mitochondrial thymidine kinase are found in severe mitochondrial DNA depletion myopathy (*9*). In addition, upregulated activity of this enzyme has been found in a patient who suffered from mitochondrial DNA depletion and fatal infantile lactic acidosis (*9*). These mitochondrial thymidine kinase failures caused premature death before the age of four and suggest that the feedback inhibition and regulation of deoxyribonucleoside kinase activity is of significant physiological importance.

In contrast to mammals, which have four different deoxyribonucleoside kinases with distinct but overlapping specificities, the fruit fly *Drosophila melanogaster* has only one such deoxyribonucleoside kinase (dNK, EC 2.7.1.145) with the ability to phosphorylate all natural deoxyribonucleosides with outstanding high efficiencies (*10*, *11*). Besides all four deoxyribonucleosides, the enzyme phosphorylates a broad variety of nucleoside analogues. The three-dimensional structure of dNK has recently been determined and provided the basis for further understanding of the structure−function relationship among the deoxyribonucleoside kinases (*12*).

A mode of feedback inhibition has been proposed for the inhibition of human deoxycytidine kinase (dCK) by its

† This work was supported by grants from the Swedish Natural Science Research Council (to H.E.), the Swedish Strategic Research Foundation (to H.E.), and the Swedish Cancer Foundation (to H.E.) and by grants from the Danish Research Council and the John and Birthe Meyer Foundation (to J.P.) and the NOVO research foundation and the Danish Research Council (to B.M.P.).

* To whom correspondence should be addressed.
‡ Swedish University of Agricultural Sciences.
§ Technical University of Denmark.
|| Roskilde University.
⊥ Present address: AstraZeneca R&D Mölndal, S 43183 Mölndal, Sweden.

[1] Abbreviations: dNK, deoxyribonucleoside kinase *Drosophila melanogaster* (dNK, EC 2.7.1.145); dGK, deoxyguanosine kinase; dCK, deoxycytidine kinase; dT, deoxythymidine; dC, deoxycytidine; dNTP, deoxyribonucleoside triphosphate; dNDP, deoxyribonucleoside diphosphate; dNMP, deoxyribonucleoside monophosphate; rmsd, root-mean-square deviation.

10.1021/bi0340043 CCC: $25.00
Published on Web 04/25/2003

feedback inhibitor dCTP (*5*). In that study, the end-product dCTP exhibited competitive inhibition against ATP with a dissociation constant estimated to be 0.7 μM. On the basis of the kinetic results and on the strong and specific inhibition by dCTP, it has been proposed that this end product acts as a bisubstrate analogue with its triphosphate group binding to the phosphate donor site of the enzyme and its deoxycytidine moiety overlapping and binding to the deoxyribonucleoside site in a highly specific manner. The favorable interaction with the nucleoside moiety in addition to the strong binding of the triphosphate part would make deoxyribonucleotides potent inhibitors (*13*). Further support for such a mechanism has been given by the crystal structure of human deoxyguanosine kinase (dGK), which has added more insight into the molecular basis of the feedback inhibition (*12*). dGK was cocrystallized with adenosine triphosphate (ATP), which was found to bind with the base and sugar in the substrate site and with the phosphates partly occupying the phosphate donor site. It should be stressed that, in this case, it was not the deoxyribonucleoside triphosphate, but the ribonucleoside triphosphate, that has the additional hydroxyl group at the 2′ position, bound to the enzyme. Despite the fact that ATP itself is not a metabolic inhibitor, ATP bound to dGK seems so far to be a good model to understand the molecular mechanisms behind the feedback regulation of the pathway.

To further investigate the feedback mechanism, we crystallized dNK in the presence of its substrate dT or its feedback inhibitor dTTP and determined the structure of the two complexes. The obtained data provide a simple and plausible model showing that feedback inhibition of the pathway operates through binding of the end-product to the phosphate acceptor site and partially to the phosphate donor site of dNK. The study also demonstrates that the binding of the inhibitor gives rise to conformational changes connected to a Mg^{2+}-ion bound to the inhibitor's phosphates and catalytically important residues of the enzyme.

MATERIALS AND METHODS

Protein Purification and Kinetic Studies. The expression and purification of the recombinant wildtype and truncated *D. melanogaster* dNK have been described (*10*). The construction, expression, and purification of the M88R/A110D *D. melanogaster* dNK have been described (*7*, *8*). Nucleoside kinase activity measurements and determination of inhibition constants were done as described previously (*6*).

Kinetic Investigations. Enzyme kinetic data were evaluated as described previously by nonlinear regression analysis using the Michaelis−Menten equation $v = V_{max}[S]/(K_m + [S])$ with one variable substrate and the other substrate at a fixed saturating concentration (*7*). Inhibitor concentrations giving 50% inhibition of enzyme activity (IC_{50}) were determined by fitting the initial velocities to the equation $v_I = v_0/(1 + [I]/IC_{50})$ in the presence of varying inhibitor concentrations [I] at the indicated substrate concentrations. v_I and v_0 are the velocities in the presence or absence of inhibitor, respectively. To determine the type of inhibition, the apparent V_{max} and K_m values were determined at three different inhibitor concentrations and compared to V_{max} and K_m for the uninhibited enzymatic reaction. Once an inhibition pattern was established, the entire data set were fitted to the appropriate equation:

competitive inhibition,

$$v = V_{max}[S]/\{K_m(1 + [I]/K_{ic}) + [S]\}$$

uncompetitive inhibition,

$$v = V_{max}[S]/\{K_m + (1 + [I]/K_{iu})[S]\}$$

mixed inhibition,

$$v = V_{max}[S]/\{K_m(1 + [I]/K_{ic}) + (1 + [I]/K_{iu})[S]\}$$

K_{ic} is the competitive inhibition constant, and K_{iu} is the uncompetitive inhibition constant.

Crystallization. Crystals of the dNK−dT complex and the dNK−dTTP complex were grown by the vapor diffusion method with hanging drops. The crystallization solution consisted of 0.1 M MES pH 6.5, 0.2 M ammonium sulfate, 18−22% (W/V) mPEG5000, and 5−10% (W/V) PEG400. The crystallization solution was mixed in equal volumes with the enzyme solution, which apart from 5 to 10 mg mL^{-1} protein contained 5 mM dT or dTTP. The solutions were then left to equilibrate at 14 °C and the crystals grew typically in 3−5 days to a size of 100 × 50 × 50 μm^3 for dNK−dTTP and 150 × 50 × 50 μm^3 for dNK−dT.

Data Collection. X-ray diffraction data for the dNK−dT and dNK−dTTP complexes were collected at 100 K on beamline ID14/EH1 and ID14/EH2 at ESRF in Grenoble, France, using a ADSC Q4 CCD detector. The data for dNK−dT were scaled and merged using the programs Mosflm (*14*) and Scala (*15*). The crystals belong to the monoclinic space group $P2_1$ and have a solvent content of 43.5%, which corresponds to four dimers in the asymmetric unit. The data for dNK-dTTP were indexed, scaled, and merged using the programs Denzo and Scalepack (*16*). The crystals belong to the monoclinic space group $P2_1$. They have a solvent content of 48%, which corresponds to two dimers in the asymmetric unit. Data collection statistics are shown in Table 1.

Table 1: Data Collection and Refinement Statistics for the dNK−dTTP and dNK−dT Complexes

	dNK dT	dNK dTTP
space group	$P2_1$	$P2_1$
cell dimensions (Å)	$a = 70.4$, $b = 71.2$, $c = 226.3$ $\beta = 90.6°$	$a = 67.1$, $b = 119.9$, $c = 60.5$ $\beta = 92.9°$
content of the asymmetric unit	four dimers	two dimers
resolution range (Å)	70−2.5	25−2.4
completeness (%)	90.4 (68.1)[a]	99.6 (98.9)[a]
R-sym (%)	5.0 (23.6)[a]	6.2 (22.9)[a]
$I/\sigma I$	8.0 (1.8)[a]	21.9 (4.2)[a]
redundancy	2.1 (1.8)[a]	5.5 (3.0)[a]
no. of unique reflections	70 001	42 341
beamline	ID14/EH1 ESRF	ID14/EH2 ESRF
temp (K)	100	100
R factor (%)	22.7	22.0
R_{free} (%)	27.6	24.2
rmsd bond lengths (Å)	0.007	0.011
rmsd bond angles (°)	0.994	1.404
mean B value (Å^2)	34	35

[a] Numbers in parentheses indicate the outer resolution bin: dT 2.64−2.5 and dTTP 2.49−2.40

Structure Determination and Refinement. The structure of the dNK−dT complex was solved by molecular replacement using the program Molrep (*17*), and the refined structure of the previously solved dNK−dC dimer was used as a search model. After rigid-body refinement in Refmac5 (*18*) and constrained refinement in CNS (*19*), an initial electron density map was calculated. From this map, most of the polypeptide chain could be built using the program O (*20*). The asymmetric unit containing four dimers allowed constrained 8-fold noncrystallographic averaging throughout the refinement.

The structure of the dNK−dTTP complex was solved by the molecular replacement method using the program AMoRe (*21*). The coordinates of the refined dNK−dC monomer were also here used as a search model. After rigid-body refinement and one round of simulated annealing in CNS (*19*), an initial electron density map was calculated. From this map, most of the polypeptide chain could be built using the program O (*20*). Refinement was carried out using the program CNS (*19*) including simulated annealing, energy minimization, and individual atom B-factor refinement. The presence of two dimers in the asymmetric unit allowed restrained 4-fold noncrystallographic averaging throughout the refinement. Refinement statistics are summarized in Table 1.

Coordinates: The atomic coordinates and structure factors of the dNK−dTTP and dT complexes have been deposited at the Protein Data Bank (codes 1oe0, 1ot3).

RESULTS

Structure Determination and Quality of the Structures. The structure of the dNK−dT and dNK−dTTP complexes were determined on the same recombinant C-terminal truncation mutant that lacks the last 20 residues that was used for the structure determination of the enzyme with its substrate deoxycytidine (dNK−dC) (*12*). The dNK−dT complex structure has been refined at 2.5 Å resolution to an R-factor of 22.7 and an R_{free} of 27.6 and the dNK−dTTP complex structure at a resolution of 2.4 Å to a final R-factor of 22.0% and an R_{free} of 24.2% with good stereochemistry in both cases, see Table 1.

Both the N- and C-termini of dNK are flexible in all structures and the loop 195−199 in some molecules. In the final electron density of both dNK−dT and dNK−dTTP complexes, the first 11 residues could not be localized. This means that six more residues were visible compared to the dNK−dC complex structure. At the C-terminus, about 20 residues were not visible in the electron density maps for all complexes. Arg105 is outside the preferred regions of the Ramachandran plot in all molecules. This residue has good density and its guanidino group makes contacts with the α-phosphate oxygen of the inhibitor in the dTTP complex and Glu52 and O5′ in the substrate complexes.

The electron densities for dT and dTTP are strong and the substrate and inhibitor could easily be fitted in difference maps (Figure 1). There is also additional density close to the β- and γ- phosphates of dTTP which has been interpreted as a magnesium ion and has been refined as such. In the dNK−dT complex, density for a sulfate ion is present in the P-loop in all eight subunits in the crystals. Furthermore, an additional sulfate ion is bound between two of the dimers

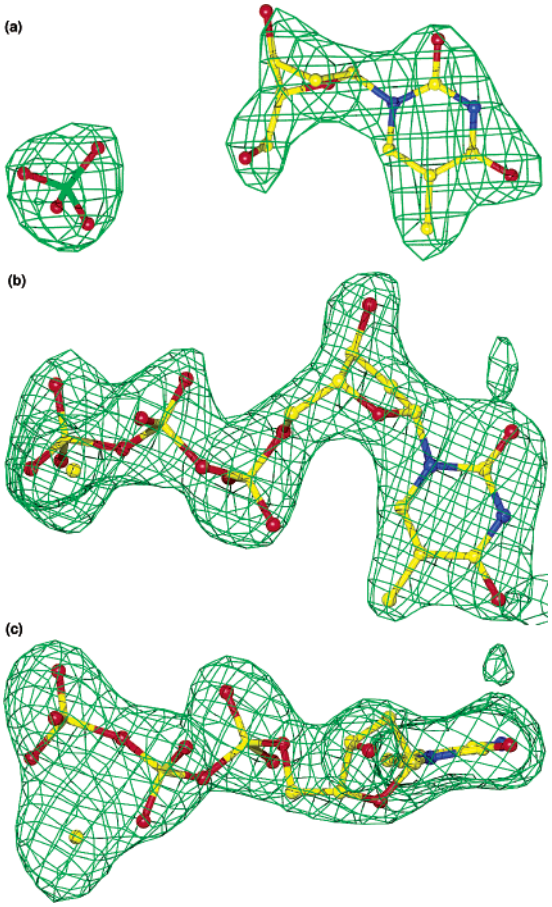

FIGURE 1: (a) Difference electron density ($F_o - F_c$) map for dT and sulfate contoured at 3σ. (b) Difference electron density ($F_o - F_c$) map for dTTP contoured at 3σ. (c) Difference electron density shown perpendicular to panel b demonstrating the density for Mg^{2+}- (yellow sphere).

in the asymmetric unit. This causes Arg169 to point outward against the neighboring dimer in two subunits instead of inward toward the phosphate donor site as seen in the other six subunits of the dNK−dT complex and in all subunits in the dNK−dTTP structure complex.

Structure of the dNK−dT Substrate Complex. dNK is a dimeric molecule with a five stranded α/β subunit structure similar to other deoxyribonucleoside and deoxyribonucleotide kinases (Figure 2). The dNK−dT complex is very similar to the dNK−dC complex (*12*). Both structures contain a sulfate ion bound in the P-loop and the substrates are located at similar positions. The interactions of the deoxyribose and base (Figure 3a) are the same with two exceptions. First, the amide group of Gln81 is differently oriented in the two complexes (a χ_3 rotation of about 180°). In the dNK−dT complex, its carbonyl group forms a hydrogen bond to N3 and its amino group forms a hydrogen bond to the oxygen at 4-position of the base. In the dC complex, the amino group of Gln81 forms a hydrogen bond to N3 and its carbonyl group to the amino group in the 4-position. Second, the methyl group in thymine has expelled two water molecules from the binding site and instead has hydrophobic interactions with the hydrophobic part of Arg105 and with Val84, Met88, and Ala110.

The eight subunits in the asymmetric unit are very similar, and the refinement was performed using constrained noncrystallographic symmetry. However, the LID region be-

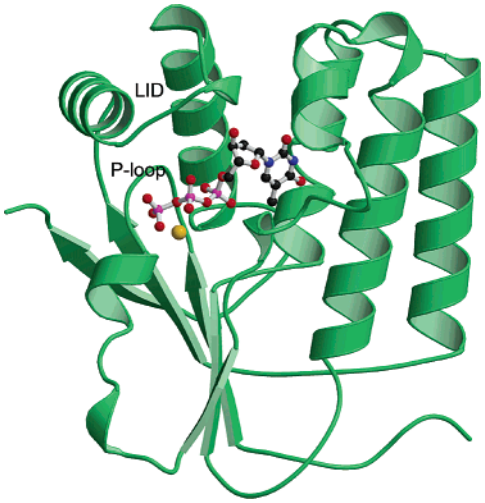

FIGURE 2: dNK subunit (in green) with bound dTTP inhibitor. The yellow sphere represents the magnesium ion. Figures 2−6 were made using MOLSCRIPT (*24*).

tween residues 163 to 169 and the loop between residues 194 to 201 is distinctly different in the monomers of dNK−dT and was therefore excluded from the noncrystallographic symmetry constrained refinement.

Structure of the dNK−dTTP−Mg Ternary Complex. The overall structure of the dNK−dTTP complex is practically identical to the complexes with deoxycytidine and deoxythymidine except in a few places, most importantly in the phosphate binding region (see below). The N-terminal residues of the dNK−dTTP complex are close to the dimer interface and residues 13−14 of each subunit contact each other as in the dT-complex. This was not seen in the dC complex, though the difference is most likely due to changed packing of the molecules in the crystal.

The four subunits in the asymmetric unit are very similar, and the refinement was performed using restrained noncrystallographic symmetry. However, the loop between residues 192 to 201 is distinctly different in the monomers of dNK−dTTP and was therefore excluded from the restrained noncrystallographic symmetry refinement. The final monomer structures can be superimposed on each other with rmsd values of 0.17−0.39 Å comparing all Cα atoms of the four subunits. The differences are restricted to the loop residues 192−201.

dTTP Interactions with dNK. The long substrate cleft is located perpendicular to the C-termini of the parallel β-sheet (Figure 2) and dTTP binds with the base at the substrate site located deep in the protein (Figure 2). The nucleoside part of dTTP is anchored by two hydrogen bonds to the base and two to the deoxyribose (Figure 3b). The thymine base makes two hydrogen bonds to Gln81 in the same manner as in the dNK−dT complex. The carbonyl oxygen in 2-position is hydrogen bonded to a water molecule that also binds to Tyr179 and Tyr70, which in turn is hydrogen bonded to the 3′-oxygen of the deoxyribose. On the opposite side of the base, the methyl group at C5 of the thymine binds in a hydrophobic pocket formed by Trp57, Val84, Ala110 and the hydrophobic part of Arg105 (Arg105 binds with its guanidino group to the α-phosphate of the inhibitor). The 3′-OH of the deoxyribose is hydrogen bonded to Tyr70 and Glu172. The sugar ring is in 2′-endo conformation.

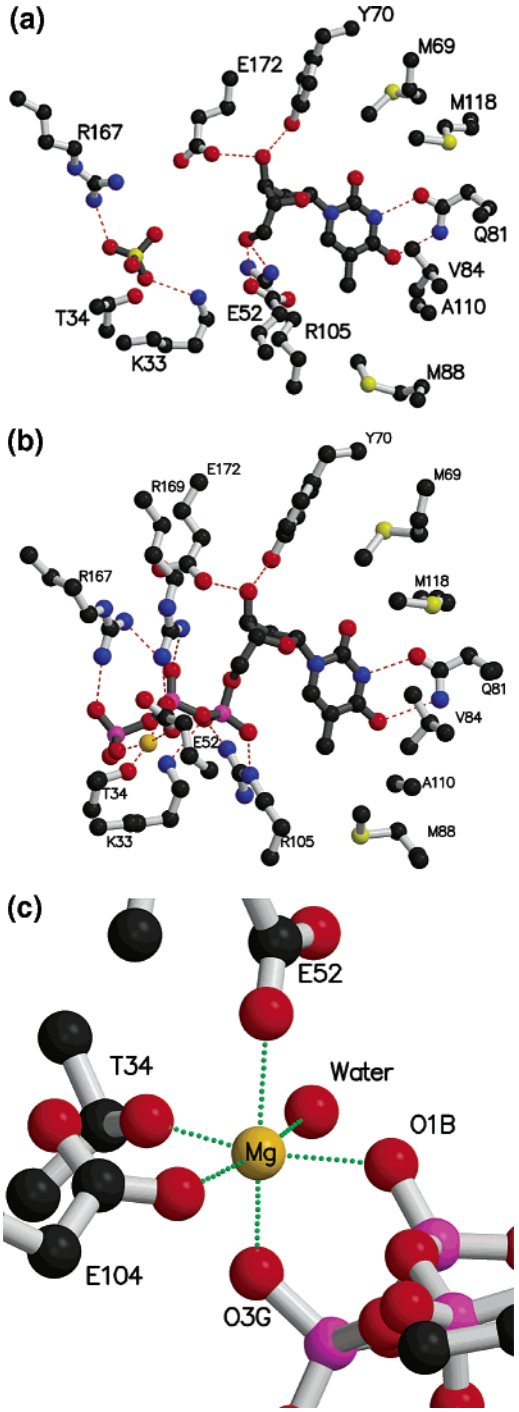

FIGURE 3: Binding at the active site of (a) dT and a sulfate ion (b) dTTP. Hydrogen bonds are shown as dotted red lines. Trp57 on top of the base has been omitted for clarity. (c) Mg-coordination to the dTTP phosphate oxygens (to the right), protein atoms and a water molecule.

The triphosphate part of the inhibitor is bound by a large number of hydrogen bonds between the phosphate oxygens and the enzyme (Figure 3b). The γ-phosphate is bound to the P-loop main chain as well as Arg 167. The β-phosphate is bound to both Arg167 and Arg169. The α-phosphate is bound to both Lys33 and Arg105. The O3 of the γ-phosphate and the O1 of the β-phosphate coordinates a magnesium ion, which together with Glu52 OE2 and Thr34 OG, form a square plane in an almost perfect octahedron with Glu104 OE2 and a water molecule at the two remaining vertexes (Figure 3c). The magnesium−ligand distances are 2.0−2.3

FIGURE 4: Stereo figure showing the conformational changes around the substrate site with the dNK−dC complex in yellow and the dNK−dTTP complex in green. The side-chain of Glu52, which coordinates the magnesium ion in the dTTP complex, is shown in ball-and-stick.

Å. The interacting Arg167 and Arg169 are located in the LID region, Lys33 is located in the P-loop, and the Glu104−Arg105 pair is located in the connection between the third strand of the sheet and the following helix (*12*). These residues are all conserved among this group of eukaryotic deoxyribonucleoside kinases (*12*).

Comparison of the Inhibitor Complex with the Substrate Complexes. The position in the active site of the deoxyribose and thymine part of the inhibitor is very similar to that of the sugar and base of dT and dC in the substrate complexes, and the interactions are practically identical. Differences between those atoms of the bases of the inhibitor and the substrate that are located furthest into the active site are roughly about 0.5 Å apart in the two structures, depending how the superposition is done. The position of the deoxyribose moieties deviates slightly more, about 1 Å.

The dNK−dT complex structure was determined from crystals with a sulfate ion present in the P-loop of the phosphate donor site, and it is generally very similar to the dNK−dTTP complex and differences in the P-loop in the two cases are generally less than 1 Å. The structure of the LID region in the different peptide chains in the dNK−dT complex demonstrate that it has some flexibility and its structure was influenced by packing interactions in the crystals mediated by sulfate ions in two of the subunits. The Cα of Arg169 differ by 4 Å and the tip of the side chain by 15 Å in the two cases. When the dT and dTTP complexes are compared, some conformational changes in the order of 1−2 Å are found in the LID region. In addition, there is a major conformational change of the region between residues 51−56 (Figure 4). Glu52, which has been suggested to be involved in the catalysis and acts as a base in the initial 5′-OH activation of the deoxyribonucleoside, has shifted from its position and instead of hydrogen bonding to the 5′-OH of the deoxyribose as in the dT complex, the side chain in the dTTP complex is now coordinating the Mg-ion and the side chain has moved 6.5 Å. As a consequence, the main chain of residues 52−53 has moved 2−3 Å. A difference occurs also for the guanidino group of Arg105, which binds to Glu52 in the dT complex but to the α-phosphate in the dTTP inhibitor complex.

The *β*- and *γ*-phosphates of the dTTP inhibitor bind strongly to the enzyme. Beside the interactions through the magnesium ion, eight hydrogen bonds are formed to the main chain and Lys33 of the P-loop, as well as Arg167 and Arg169 in the LID-region.

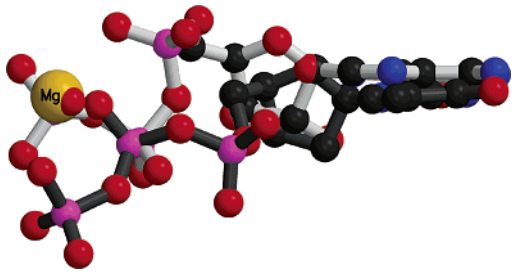

FIGURE 5: Comparison of dTTP bound to dNK (in black bonds) with ATP (in white bonds) binding to dGK when the proteins have been superimposed.

Comparison with the dGK−ATP Complex. The structure of human deoxyguanosine kinase with ATP (dGK-ATP), which has so far been the structural model for the feedback inhibition of the deoxyribonucleoside kinases (*12*), has several similarities with the present dNK−dTTP complex structure. The general mode of binding with the base located in the substrate base site is similar and the position of the base and deoxyribose is essentially the same in the two cases (Figure 5). However, phosphate binding differs significantly between the ATP and dTTP complexes. The *β*-phosphate is located at roughly the same position in the two cases, whereas the α- and *γ*-phosphates differ considerably (Figure 5). Despite its presence in the crystallization media, there was no significant density for a magnesium ion in the dGK−ATP complex and the conformation of the region corresponding to residues 51−56 is similar to that of the dNK−dC and dNK−dT complexes. This suggests that the presence of the magnesium ion is important for the observed conformational change.

The phosphate site in the two inhibitor complexes overlaps with the phosphate binding site for the phosphate donor, which usually is ATP. The best model for a phosphate donor can be constructed from the related *Herpes simplex* virus thymidine kinase structure with the reaction products ADP and dTMP (*22*). Comparing with the inhibitor complex, the *γ*-phosphate of dTTP in the inhibitor complex is located roughly at the *β*-phosphate of the ADP product whereas the α-phosphate of dTTP overlaps roughly with the phosphate of the product dTMP of the Herpes enzyme complex (Figure

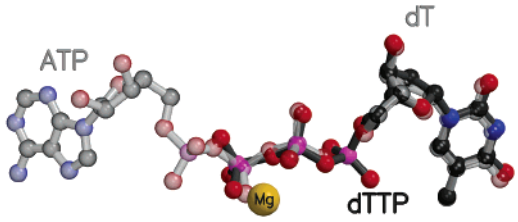

FIGURE 6: Comparison of dTTP (in black bonds) with the substrate dT (in white bonds) bound to dNK and a modeled ATP based on ADP and dTMP from a superimposed *Herpes simplex* thymidine kinase complex.

6). The feedback inhibitor thus occupies both the substrate site and the phosphate donor site and acts as a bisubstrate inhibitor.

Kinetic Investigations. To test if the crystal structure presented here is in accordance with the kinetic behavior, and that the binding of dTTP as shown here does not represent an artifact due to high dTTP concentration in the crystallization solution, we first verified that the truncated dNK (rDm-dNKΔC20) behaved like the wild type enzyme (rDm-dNK) with respect to the substrate affinity and inhibition by dTTP. The truncated dNK has basically unchanged apparent K_m values for both the phosphate donor, ATP (5.2 μM for rDm-dNK and 3 μm for rDm-dNKΔC20), and acceptor, dT (1.2 μM for rDm-dNK and 1.7 μM for rDm-dNKΔC20). However, the rDm-dNKΔC20 k_{cat} is increased and the enzyme more stable than the full-length protein (*10*). For wildtype-dNK, we previously found dTTP to be a competitive inhibitor with respect to ATP (K_{ic} = 5.3 nM) and a predominantly uncompetitive inhibitor with respect to dT with inhibitor constants in the micromolar range (K_{ic} = 16.3 μM, K_{iu} = 4.7 μM) (*7*). For rDm-dNKΔC20, we found the dTTP feedback inhibition mode unchanged, since the inhibition toward ATP was competitive (K_{ic}= 40 nM) and predominantly uncompetitive toward thymidine (K_{ic} = 34 μM and K_{iu} = 6 μM).

In the following, it was tested if dTTP interacts with the hydrophobic pocket at the nucleoside binding site as observed in the crystal structure and deduced from the kinetic and inhibition experiments. The ability of dTTP to work as a phosphate donor instead of inhibiting the phosphorylation of dT was tested on a double mutant M88R/A110D. This mutant has a modified nucleoside binding site interfering with the 5-methyl group of the thymine base (*8*). According to the crystal structure presented here, the mutations should also hinder proper binding of dTTP as an inhibitor. In the inhibition experiments with dT as phosphate acceptor (10 μM dT, 2.5 mM ATP) dTTP gave an IC_{50} value of 6.9 μM for the wild-type dNK (*7*), while for the double mutant at the same substrate concentrations, there was no inhibition of dT phosphorylation with dTTP concentrations up to 1000 μM (data not shown). In contrast to this, the double mutant M88R/A110D can use dTTP as phosphate donor with both nucleoside substrates, dT and dC (Table 2). Other triphosphates were used in parallel as controls. This clearly demonstrates that specific modifications within the nucleoside binding site abolish the ability of dTTP to act as an inhibitor and shows that the nucleoside binding site is involved in the dTTP-mediated feedback inhibition of dNK.

Table 2: Relative Activity of Wildtype dNK and M88R/A110D with Different Phosphate Donors at 100 μM and dC or dT at 10 μM

	dT		dC	
	M88R/A110D	wildtype-dNK	M88R/A110D	wildtype-dNK
ATP	100[a]	100	100	100
CTP	98	94	218	108
UTP	15	71	136	62
GTP	13	39	89	78
dATP	135	107	469	92
dCTP	85	153	81	21
dGTP	10	176	69	26
dTTP	35	n.d.[b]	63	n.d.

[a] The relative activity with ATP was set to 100% for each enzyme. [b] n.d. = not detectable.

DISCUSSION

Recent findings on subactive or overactive deoxyribonucleoside kinases associated with severe human diseases (*9*, *23*) suggest that precise regulation of the nucleoside salvage pathway is of significant physiological importance. In this study, we provide the structural basis to understand the molecular mechanisms behind feedback inhibition of the deoxyribonucleoside salvage pathway using *Drosophila* dNK as a model.

dNK was cocrystallized with its substrate dT as well as with its feedback inhibitor dTTP and a Mg-ion. Small conformational changes in the P-loop and the LID region were observed, where conformational changes were expected. In the LID region, Arg167 and Arg169 that binds to the phosphates of the dTTP in the inhibitor complex are more loosely organized in the dT substrate complex. This is observed as a much weaker density for this region in the dT complex compared to the dTTP complex. Binding of a second sulfate ion between two of the dimers in the asymmetric unit of the dT complex stabilizes the LID region between these two molecules and allows for good density for Arg167 and Arg169 in two of the subunits in the asymmetric unit (A and H). This is not the case for the rest of the subunits where the electron density is too weak to accurately locate all arginines.

A major conformational change is observed in the region between residues 51−56 (Figure 4). A Mg ion was found to be involved in these changes. Glu52, which has been suggested to be involved in the catalysis by acting as the base in the initial activation of the 5′-OH of the deoxyribonucleoside (*12*), has shifted from its position and instead of hydrogen bonding to the deoxyribose 5′-OH, it has moved 6.5 Å and is now coordinating the Mg ion. This means that deactivation of dNK after dTTP binding involves not only steric hindrance at the substrate binding site but also a displacement of the catalytic base.

In the structure presented here, dTTP binds to dNK as a bisubstrate inhibitor. This multisubstrate binding model provides a simple and plausible explanation for the highly specific and effective feedback inhibition of dNK by dTTP. Moreover, it is in accordance with the observed competitive inhibition by dTTP with respect to ATP. If dTTP was bound only to the phosphate donor binding site, it should be able to serve as a phosphate donor, which is not the case (*7*, *8*) (Table 2). Moreover, such a model would not explain that dTTP (K_{ic} = 40 nM) binds almost 100 times stronger to the enzyme than ATP (K_m = 3 μM).

Recently, several mutants with altered nucleoside binding site of dNK have been generated by site-directed mutagenesis (*7*, *8*). The dT phosphorylation by the dNK double mutant M88R/A110D was decreased about 850000-fold, compared to only 1000−3000-fold decrease in the phosphorylation efficiency with the other three natural substrates (*7*, *8*). In contrast to wildtype-dNK, this double mutant can use dTTP as phosphate donor (Table 2) and is not inhibited by dTTP. This shows that mutations in the nucleoside base binding pocket affect not only substrate specificity but also the recognition of the feedback inhibitor. This is consistent with the binding of dTTP in the crystal structure so that dTTP can act as a bisubstrate inhibitor simultaneously binding with its base in the nucleoside binding pocket of the enzyme and its phosphate groups in the phosphate donor pocket. Discrimination against the dT base, as displayed by the dNK double mutant M88R/A110D, also results in discrimination against dTTP, which now acts as a phosphate donor instead of an inhibitor, binding at the ATP site.

There must, however, be a very delicate balance between the situations when a dNTP binds as a feedback inhibitor and when it acts as a phosphate donor. dNK is a multisubstrate nucleoside kinase that is active with the same k_{cat} for all four deoxyribonucleosides. According to the k_{cat}/K_m values, dT is the best substrate but only about twice as good as dC. It is thus surprising in view of the small differences for the deoxynucleoside substrates, that dCTP is a very good phosphate donor but a poor inhibitor (*7*). Thymine is more hydrophobic than cytosine and should be less favorable in the exposed base binding site of the phosphate donor site and dTTP should have slightly lower affinity at this site than dCTP. However, this effect cannot be large since dTTP is only slightly less efficient than dCTP as phosphate donor for the double mutant (Table 2).

Taken together, the obtained structural and kinetic data convincingly demonstrate that feedback inhibition of the model deoxynucleoside kinase, dNK, operates through binding of the end-product of the salvage pathway to the nucleoside substrate site and partially to the phosphate donor site of dNK. In addition, end-product-inhibition of human deoxycytidine kinase (*5*), bacterial deoxyguanosine kinase (*4*), and human deoxyguanosine kinase (*12*) by the respective dNTP was postulated to occur because the dNTP behaved like a bisubstrate analogue as derived from kinetic or structural evidence. This suggests that inhibition of a deoxyribonucleoside kinase by its end-product dNTP acting as a bisubstrate analogue as shown here is a general mechanism operating in deoxyribonucleoside kinases.

ACKNOWLEDGMENT

We would like to thank Malin Uppsten for assistance with the crystallographic studies and Michael Sandrini for help with the double mutant M88R/A110D.

REFERENCES

1. Thelander, L., and Reichard, P. (1979) Reduction of ribonucleotides. *Annu. Rev. Biochem. 48*, 133−158.
2. Arnér, E. S. J., and Eriksson, S. (1995) Mammalian deoxyribonucleoside kinases. *Pharmacol. Ther. 67*, 155−186.
3. Jordan, A., and Reichard, P. (1998) Ribonuclotide reductases. *Annu. Rev. Biochem. 67*, 71−98.
4. Andersen, R. B., and Neuhard, J. (2001) Deoxynucleoside kinases encoded by the yaaG and yaaF genes of *Bacillus subtilis*. Substrate specificity and kinetic analysis of deoxyguanosine kinase with UTP as the preferred phosphate donor. *J. Biol. Chem. 276*, 5518−5524.
5. Kim, M. Y., and Ives, D. H. (1989) Human deoxycytidine kinase: kinetic mechanism and end product regulation. *Biochemistry 28*, 9043−9047.
6. Knecht, W., Munch-Petersen, B., and Piškur, J. (2000) Identification of residues involved in the specificity and regulation of the highly efficient multisubstrate deoxyribonucleoside kinase from *Drosophila melanogaster*. *J. Mol. Biol. 301*, 827−837.
7. Knecht, W., Petersen, G. E., Munch-Petersen, B., and Piškur, J. (2002) Deoxyribonucleoside kinases belonging to the thymidine kinase 2 (TK2) -like group vary significantly in substrate specificity, kinetics and feed-back regulation. *J. Mol. Biol. 315*, 529−540.
8. Knecht, W., Sandrini, M. B. P., Johansson, K., Eklund, H., Munch-Petersen, B., and Piškur, J. (2002) A few amino acid substitutions can convert deoxyribonucleoside kinase specificity from pyrimidines to purines. *EMBO J. 21*, 1873−1880.
9. Saada, A., Shaag, A., Mandel, H., Nevo, Y., Eriksson, S., and Elpeleg, O. (2001) Mutant mitochondrial thymidine kinase in mitochondrial DNA depletion myopathy. *Nat. Genet. 29*, 342−344.
10. Munch-Petersen, B., Knecht, W., Lenz, C., Sondergaard, L., and Piškur, J. (2000) Functional expression of a multisubstrate deoxyribonucleoside kinase from *Drosophila melanogaster* and its C-terminal deletion mutants. *J. Biol. Chem. 275*, 6673−6679.
11. Munch-Petersen, B., Piškur, J., and Sondergaard, L. (1998) Four deoxynucleoside kinase activities from *Drosophila melanogaster* are contained within a single monomeric enzyme, a new multifunctional deoxynucleoside kinase. *J. Biol. Chem. 273*, 3926−3931.
12. Johansson, K., Ramaswamy, S., Ljungcrantz, C., Knecht, W., Piškur, J., Munch-Petersen, B., Eriksson, S., and Eklund, H. (2001) Structural basis for substrate specificities of cellular deoxyribonucleoside kinases. *Nat. Struct. Biol. 8*, 616−620.
13. Park, I., and Ives, D. H. (1995) Kinetic mechanism and end-product regulation of deoxyguanosine kinase from beef liver mitochondria. *J. Biochem (Tokyo) 117*, 1058−1061.
14. Leslie, A. G. W. (1994) *Mosflm User Guide: Mosflm version 5.20*, MRC Laboratory of Molecular Biology, Cambridge, UK.
15. CCP4. (1994) The CCP4 Suite: Programs for Protein Crystallography, *Acta Crystallogr. D50*, 760−763.
16. Otwinowski, Z., and Minor, W. (1997) Processing of X-ray data collected in oscillation mode, in *Methods in Enzymology, Macromolecular Crystallography, Part A*, (Carter, C. W., Jr., Sweet, R. M., Eds.) pp 307−326, Academic Press, New York.
17. Vagin, A., and Teplyakov, A. (1997) MOLREP: an automated program for molecular replacement. *J. Appl. Crystallogr. 30*, 1022−1025.
18. Murshudov, G. N., Vagin, A. A., and Dodson, E. J. (1997) Refinement of macromolecular structures by the maximum-likelihood method. *Acta Crystallogr. D53*, 240−255.
19. Brünger, A. T., Adams, P. D., Clore, G. M., DeLano, W. L., Gros, P., Grosse-Kunstleve, R. W., Jiang, J. S., Kuszewski, J., Nilges, M., Pannu, N. S., Read, R. J., Rice, L. M., Simonson, T., Warren, G. L. (1998) Crystallography & NMR system: a new software suite for macromolecular structure determination. *Acta Crystallogr. D 54*, 905−921.
20. Jones, T. A., Zou, J. Y., Cowan, S. W., and Kjeldgaard, M. (1991) Improved methods for building protein models in electron density maps and the location of errors in these models. *Acta Crystallogr. 47*, 110−119.
21. Navaza, J. (1994) AMoRe: an automated package for molecular replacement. *Acta Crystallogr. 50*, 157−163.
22. Wild, K., Bohner, T., Folkers, G., and Schulz, G. E. (1997) The structures of thymidine kinase from *Herpes simplex* virus type 1 in complex with substrates and a substrate analogue. *Protein Sci. 6*, 2097−2106.
23. Mandel, H., Szargel, R., Labay, V., Elpeleg, O., Saada, A., Shalata, A., Anbinder, Y., Berkowitz, D., Hartman, C., Barak, M., Eriksson, S., and Cohen, N. (2001) The deoxyguanosine kinase gene is mutated in individuals with depleted hepatocerebral mitochondrial DNA. *Nat. Genet. 29*, 337−341.
24. Kraulis, P. (1991) MOLSCRIPT: a program to produce both detailed and schematic plots of protein structures. *J. Appl. Crystallogr. 24*, 946−950.

BI0340043